ISSN 1674-1056
http://cpb.iphy.ac.cn
http://iopscience.iop.org/cpb
中国物理 B
Chinese Physics
中国物理 Chinese Physics B

Evaporation of saline colloidal droplet and deposition pattern

Hong-Hui Sun(孙弘辉)[1,3], Wei-Bin Li(李伟斌)[1,3], Wen-Jie Ji(纪文杰)[1,2], Guo-Liang Dai(戴国亮)[1,3], Yong Huan(郇勇)[2,3], Yu-Ren Wang(王育人)[1,3], Ding Lan(蓝鼎)[1,3]

Citation: Chin. Phys. B . 2020, 29(1): 014701 . **doi:** 10.1088/1674-1056/ab5782
Journal homepage: http://cpb.iphy.ac.cn; http://iopscience.iop.org/cpb

What follows is a list of articles you may be interested in

Direct simulation Monte Carlo study of metal evaporation with collimator in e-beam physical vapor deposition

Xiaoyong Lu(卢肖勇), Junjie Chai(柴俊杰)

Chin. Phys. B . 2019, 28(7): 074702 . **doi:** 10.1088/1674-1056/28/7/074702

Numerical simulation of metal evaporation based on the kinetic model equation and the direct simulation Monte Carlo method

Xiaoyong Lu(卢肖勇), Xiaozhang Zhang(张小章), Zhizhong Zhang(张志忠)

Chin. Phys. B . 2018, 27(12): 124702 . **doi:** 10.1088/1674-1056/27/12/124702

Instabilities of thermocapillary-buoyancy convection in open rectangular liquid layers

Huan Jiang(姜欢), Li Duan(段俐), Qi Kang(康琦)

Chin. Phys. B . 2017, 26(11): 114703 . **doi:** 10.1088/1674-1056/26/11/114703

Evaporation of saline colloidal droplet and deposition pattern*

Hong-Hui Sun(孙弘辉)[1,3], Wei-Bin Li(李伟斌)[1,3], Wen-Jie Ji(纪文杰)[1,2], Guo-Liang Dai(戴国亮)[1,3], Yong Huan(郇勇)[2,3], Yu-Ren Wang(王育人)[1,3], and Ding Lan(蓝鼎)[1,3,†]

[1] *National Microgravity Laboratory, Institute of Mechanics, Chinese Academy of Sciences, Beijing* 100190, *China*
[2] *State Key Laboratory of Nonlinear Mechanics (LNM), Institute of Mechanics, Chinese Academy of Sciences, Beijing* 100190, *China*
[3] *School of Engineering Sciences, University of Chinese Academy of Sciences, Beijing* 100049 *China*

(Received 24 September 2019; revised manuscript received 28 October 2019; accepted manuscript online 14 November 2019)

The dynamic process of the evaporation and the desiccation of sessile saline colloidal droplets, and their final deposition are investigated. During the evaporation, the movement of the colloidal particles shows a strong dependence on the salt concentration and the droplet shape. The final deposition pattern indicates a weakened coffee-ring effect in this mixed droplet system. The microscopic observation reveals that as evaporation proceeds, the particle motion trail is affected by the salt concentration of the droplet boundary. The Marangoni flow, which is induced by surface tension gradient originating from the local evaporative peripheral salt enrichment, suppresses the compensation flow towards the contact line of the droplet. The inhomogeneous density and concentration field induced by evaporation or crystallization can be the major reason for various micro-flows. At last stage, the distribution and crystallization of NaCl are affected by the colloidal particles during the drying of the residual liquid film.

Keywords: saline droplet, evaporation, deposition pattern, disease diagnosis

PACS: 47.55.nb, 47.55.np, 45.70.Qj **DOI:** 10.1088/1674-1056/ab5782

1. Introduction

The evaporation of the sessile droplet is a ubiquitous phenomenon in nature, and in this process, there are many physical phenomena, such as convection, pinning and de-pinning of the contact line, spreading, wetting and de-wetting.[1–4] All of these phenomena have relationship with the micro-flows in the drying droplet, which controls the heat and mass transfer. Usually, the droplet is not a pure fluid but a complex fluid which contains solid particles or soluble multi-components. So, there will be some patterns remaining on the substrate. The evaporation of sessile droplets has significant value in research and application, such as nanomaterial fabrication,[5] spray coating,[6] DNA microarray design,[7] and bio-liquid analysis.[8] For this reason, the microscopic mechanism of the evaporating droplets and the methods of controlling the dried patterns have received much attention in decades. For the colloidal droplets, Deegan *et al.* first investigated the well-known "coffee-ring effect".[9] They discovered that the faster evaporation rate at the pinned contact line is the main reason for the radial outward flow, which carries colloidal particles to form the ring-like stain at the edge. After their pioneering work, much effort has been made by researchers to regulate and control the coffee-ring effect for various practical applications. Man *et al.* proposed a theory for the multi-ring pattern of the deposits that are formed when droplets of the suspension are dried on a substrate.[10] Yunker *et al.* replaced the colloidal spheres in the droplets with ellipsoids and obtained a uniform deposition in which the coffee-ring effect is suppressed.[11] In 2001, Fisher specified the relationship between evaporative flux and direction of the radial flow inside the colloidal droplet.[12]

In recent decades, the evaporation of sessile drops of biological fluid has been studied as a potential area of interest for disease diagnosis and they tried to build the relationship between the drying patterns and health status of humans.[13] The patterns of dried blood serum from healthy people are significantly different from those from the patients suffering from different diseases, such as paraproteinemia and lung cancer.[14] Most of studies have been conducted on biological fluids and blood serum, but a few have focused on whole human blood. Rapis indicated that the morphologies of dried plasma patterns can be utilized for diagnosing metastatic carcinoma.[15] Brutin *et al.* found that the dried drop patterns of whole blood from healthy individuals and those from patients suffering from anemia and hyperlipidemia are obviously different from each other.[16] The researches mentioned above suggested that the dried blood pattern analysis can become an efficient tool for relatively easy and cheap disease diagnosis through further research effort.

However, biological liquid is a kind of complex fluids, which, besides the cells, contains multi-components, such as biomolecules, inorganic electrolytes, a lot of water, *etc*. For the complicated interactions among the various components in biological liquid droplet, it is very difficult to understand

*Project supported by the National Natural Science Foundation of China (Grant Nos. 11472275 and U1738118), the Chinese Academy of Sciences Key Technology Talent Program, and the Strategic Priority Research Program of the Chinese Academy of Sciences (Grant No. XDB22040301).

†Corresponding author. E-mail: landing@imech.ac.cn

© 2020 Chinese Physical Society and IOP Publishing Ltd

the pattern formation as the droplet dries. Even so, the researchers still do their best to find some clues, starting with a simplified version of the biological fluid consisting of one or two biological components.[17,18] Studying the simpler fluids may help us to understand the mechanisms of the pattern form in more complex fluids. Shahidzadeh-Bonn *et al.* studied the crystallization process in the droplets with different dissolved salts on different substrates.[19,20] Their researches manifest that the patterns of the salt crystal stains are influenced by not only the transport properties in the liquid but also the interfacial properties of the different crystalline phases. For the droplets of binary suspension, Chen and Mohamed studied the complex patterns formed after the evaporation of droplets containing protein and salt.[17] They proposed some theoretical explanations for the patterns obtained under different conditions. In addition, Zhang *et al.* investigated the evaporative pattern morphologies of pure DNA solution and DNA-colloid binary suspension.[18] They examined the factors for influencing the patterns with different morphologies and discussed the formation mechanism for the multi-ring pattern. Although it is not a real biological fluid, we can still acquire some information about the phenomena during the deposition of the biological material.

Here, we observe the evaporation process of saline colloidal droplets *in situ* by confocal microscopy. We try to understand that the interaction between the soluble and insoluble substance during the droplet drying. We record the dynamic process of particles motion, salt crystallization, and droplet desiccation in real time with a CCD camera. By means of comparative analysis of the acquired images, we describe the interplay between salt and colloidal particles, and we make some possible explanations. The consequences are meaningful for understanding the complex dried patterns of biological liquid droplets.

2. Materials and methods

The saline colloidal droplets were made from polystyrene (PS) colloidal particles and sodium chloride (NaCl) solution. The colloidal suspension of 10 wt% was purchased from Duke Scientific Corporation and the mean diameter of the colloidal spheres is 3.03 μm. The colloidal suspension and NaCl (AR, Xilong Scientific) was diluted with ultrapure water, which was obtained from Milli-Q Reference, to prepare the blended solution used in experiment. For comparison, various dispersions with different mass fractions of colloidal particles were prepared, and the NaCl was set to be 0.9% close to the mass fraction of NaCl in plasma.

Micropipettes were used to fetch the drop and put them on the glass slides. The volume of each droplet is limited to about 1 μL. Since the physical properties of the slides are identical, the radii of the sessile droplets nearly are same. A confocal microscope (Nikon Ti) equipped with a digital camera was utilized to observe *in situ* and record the evaporation process of droplets. The frame rate of digital camera was set to be 10 fps, which was enough for capturing the details. All the evaporation experiments were done in a conditioned environment with a temperature of about 25 °C and relative humidity of about 42%.

3. Results and discussion

3.1. Complete forming process of deposition pattern in blended droplet

The mass fraction of NaCl and PS colloidal particles are indicated by ω(NaCl) and ω(PS) respectively. For a saline colloidal droplet with ω(NaCl) equal to 0.9% and ω(PS) equal to 0.1%, figures. 1(a)–1(i) show its whole drying process in a representative area on the edge of the droplet. According to the colloidal particles' motion status, we divide the whole process into three stages. The particles move stably towards the periphery of the circular droplet by the lateral flow at the beginning of evaporation. This period is defined as stage I, which corresponds to Figs. 1(a)–1(c). Subsequently, the directional motion of the particles is disturbed by the emerging vortexes. Stage II is defined as a period from this point to the moment when almost all the particles have adhered to the substrate and now the droplet turns very thin (Figs. 1(d) and 1(e)). Finally, the particles move barely and the salt separates out until the droplet is totally dry (Figs. 1(f)–1(i)).

The colloidal particles migrate slowly toward the three-phase contact line of the droplet due to a higher evaporation flux at the edge which is called compensation flow.[21] When the particles arrive at the contact line, they are confined by the meniscus and deposit on the substrate (see movie S1 in the Supplemental material). Within the stage I, a coffee-ring forms,[9,21] and this process lasts about two and a half of minutes. At the stage II, several fast-rotating vortexes emerge in the droplet, causing the colloidal particles to more complexly move in local areas (see movie S2 in the Supplemental material). At the same time, the coffee-ring at the border has a pinning effect for the liquid on triple-phase contact line,[21] the radius of the droplet therefore barely reduces in this process. At the last stage of the drying process, the particles adhere to the substrate due to the thin liquid film, and the particles are hard to move. Now, the droplet becomes a thin liquid film with a thickness close to the diameter of a colloidal particle, and the vortexes in the droplet gradually weaken until they disappear.

The salt crystallization and rupture of the liquid film occur at the stage III (Figs. 1(f)–1(i)). From the full view of the deposition pattern, the big salt crystals are few and distributed sparsely, and some crystals look like dendritic crystals at the edge. When the salt crystals appear and grow up, the movements of the colloidal particles around the crystals

are totally different from each other. We can see that the particles are pushed away from the crystals, and sometimes are pulled close to the crystals (see movie S3 in the Supplemental material). This is caused by the change of surface tension, which will be discussed in detail later. As evaporation goes on, the liquid film begins to break when the residual solution is not enough to keep the integrity of the film. The ruptured liquid films collapse into plenty of small liquid patches, and there are several colloidal particles in them. Finally, the residual liquid films evaporate so fast that some incomplete salt crystals are left over. Figure 1(j) gives a full view about the pattern.

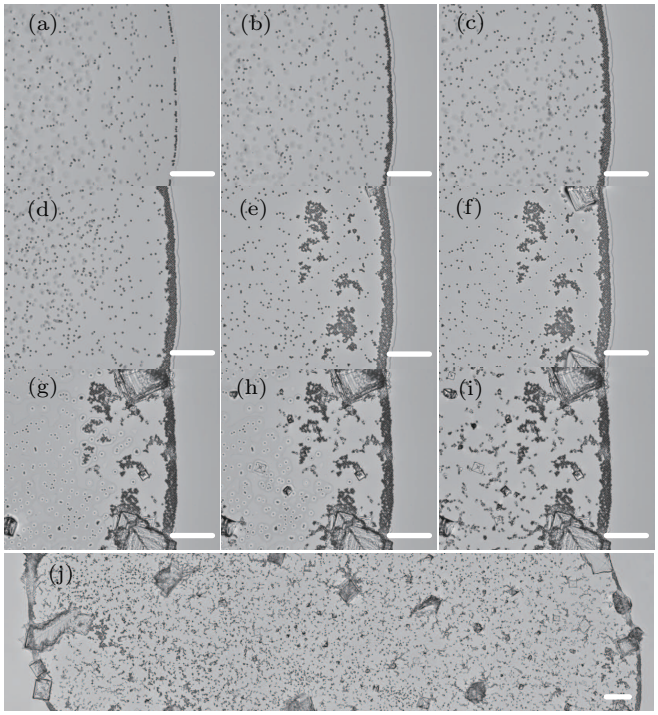


Fig. 1. (a)–(i) Drying process on the periphery of a blended droplet (ω(PS) = 0.1%, ω(NaCl) = 0.9%): (a)–(c) assembling of particles on contact line of droplet; (d) initiation of vortex; (e) all particles settled on substrate; (f) crystallization of NaCl; (g)–(h) rupture of thin liquid film and small liquid pools formation; (i) total desiccation of droplet; (j) full view of final transverse deposition. Scale bar is 100 μm.

3.2. Effects of NaCl on deposition of colloidal spheres

The salt concentration can modify the aqueous surface tension,[23] and the concentration will change during the evaporation. The local salt enrichment will induce the surface tension gradient, and the Marangoni flow will be induced which can influence the movement of the particles. At the same time, the crystalline of the salt will consume the salt in the water, and reduce the local salt concentration which will also lead to the surface tension gradient different from that mentioned above. The motion of the particles in the saline droplets is different from that in the pure colloidal droplets. We compare the movements of PS colloidal particles in these two kinds of droplets that have the same concentration of PS, to analyze how the micro-flow is affected by salt.

3.2.1. Retarding radical speed of particles

At the beginning, the colloidal particles move to the edge of the droplet for the compensation flow, and the mechanism has been clarified by Deegan.[9] Unlike the pure liquid, the salt concentration increases with the saline solution drying, and we try to understand the influence of concentration varying on the movement of the particles by checking the mean radial speeds of the particles. First, we acquire the image sequence of the area near the border of the droplet in stage I, and the frame rate is 10 fps. A series of frames are picked out in regular intervals of 60 s, beginning with the first frame. Then we pick out several typical particles from each frame. The selected particles are traced within dozens of serial frames to determine their flowing distance before they deposit at the contact line. We calculate their mean radial speeds in different time periods which can give the information about the micro-flow, and compare them to find the influence of concentration change on the particle motion. The whole process is illustrated in Fig. 2.

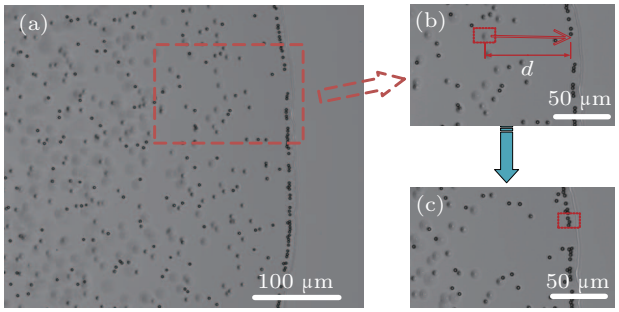


Fig. 2. Estimating the radial speed of certain particles. At a certain point in time, a typical particle was chosen and traced in a short duration around the point. The local area around it in panel (a) is magnified to see clearly in panels (b) and (c). The red frame in panel (b) shows the initial position of the particle, and panel (c) shows the final position. The displacement of the particle is denoted by d in panel (b). The time is defined by counting the frames within the interval between panel (b) and panel (c).

In stage I, there is a stable radial flow towards the edge of the droplet. Since the flow is roughly axisymmetric for circular droplets,[9] the calculated speed of the particles in a limited area near the edge is representative. It shows the intensity of compensation flow in the whole droplet. We compare the speed trend of the particles in the saline droplet with that in pure water droplet as shown in Fig. 3. The concentration of colloidal particles is kept the same in these two experimental systems. In the case of saline colloidal droplet, represented by the blue triangles in Fig. 3, the initial speed is around 6.5 μm/s. The value decreases to 5.3 μm/s in 60 s, while there is no significant change in speed after another 60 s. In the next 30 s, the speed slows down further to 4.4 μm/s. By contrast, in the case of pure colloidal droplet, represented by the red squares in Fig. 3, the speed increases from 3.7 μm/s at beginning to 18.6 μm/s seven minutes later. But the rate of increase is not uniform. In the first 4 min, the speed is increased by about 3 μm/s. While in the next 3 min, it is increased by about 12 μm/s.

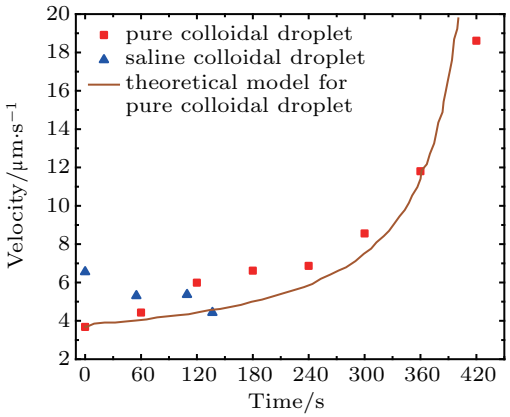


Fig. 3. Plot of radial particle speed *versus* time. The particles that are measured are about 100 μm away from the contact line. Blue triangles represent particles in blended droplet (ω(NaCl) = 0.9%, ω(PS) = 0.1%), which in pure colloidal droplet (ω(PS) = 0.1%) are represented by red squares.

Marín *et al.* described the variation of particles' radical speed inside an evaporating colloidal droplet quantitatively,[23] which will be discussed below by comparing the experimental results between two kinds of droplet systems. In this model, the height-averaged radial speed $\bar{u}$ close to the contact line is expressed as

$$\bar{u}(r,t) = \frac{D^*}{\theta(t)} \frac{1}{\sqrt{R(R-r)}}, \tag{1}$$

where $D^* = 2\sqrt{2}D_{va}\Delta c/(\pi\rho)$ represents the effect of flow driven by evaporation, with D_{va} being the diffusion constant for vapor in air, Δc the difference in vapor concentration between the drop surface and the surroundings, and ρ the liquid density. In addition, R is the contact radius of the droplet, which is determined for a certain droplet on a substrate; r is the distance from drop center; θ is the contact angle as a function of time t. For an evaporating colloidal droplet whose contact line is pinned, the evaporation follows the constant contact area mode,[24] and contact angle decreases with time t increasing in this mode. In order to make further analysis, the theoretical model actually gives the expression for $\mathrm{d}\theta/\mathrm{d}t$ by global mass conservation as follows:

$$\frac{\mathrm{d}\theta}{\mathrm{d}t} = -\frac{16D_{va}\Delta c}{\pi R^2 \rho}. \tag{2}$$

For a pure water droplet evaporating in a certain ambient environment, the parameters on the right-hand side of Eq. (2) are all constants. Thus equation (2) is equal to a constant, independent of time. The time integration of Eq. (2) is

$$\theta(t) = \frac{16D_{va}\Delta c}{\pi R^2 \rho}(t_e - t), \tag{3}$$

where t_e is the total life time of the droplet. Inserting Eq. (3) into Eq. (1), we obtain

$$\bar{u}(r,t) = \frac{\sqrt{2}R}{8(t_e - t)}\sqrt{\frac{R}{R-r}}, \tag{4}$$

where R and t_e are determined experimentally. Since the particles we measured are at a constant distance from the contact line, R–r is also determined. The theoretical curve of $\bar{u}$ varying with t is plotted in Fig. 3. The original theoretical curve is actually a bit lower than the experimental data points. For convenience, we shift the theoretical curve upward about two units to approach to the experimental data points. This does not affect the comparison results and conclusions significantly, considering the fact that the relative variation trend of speed is our main focus.

Obviously, the variation trend of speed in experimental pure colloidal droplet matches up well enough with the theoretical model. However, the speed in saline colloidal droplet has a distinct tendency, which implies that the dissolved salt plays an important role in retarding the outward flow. The theoretical model also indicates this. As the evaporation goes on in the saline colloidal droplet, the concentration of salt increases, which results in the growth of ρ. With ρ as a function of t, the integration of Eq. (2) will not be Eq. (3) any longer, and θ will not be inversely proportional to ρ. When equation (3) is inserted into Eq. (1), the parameter ρ cannot be eliminated. Consequently, the final expression of $\bar{u}$ also involves density ρ. Hence, the variation trend of $\bar{u}$ with time is influenced by the growth of ρ in blended droplet, which is definitely distinct from the curve of Eq. (4).

In fact, when the density of blended droplet, ρ increases with time, factor D^* will decrease. This can be derived from the expression of D^* and ρ. The particle speed $\bar{u}$ presents a decreasing trend in this situation, which means that the flow driven by evaporation is weakened by the increase of density. On the other hand, the particle speed $\bar{u}$ has a tendency to increase with the decrease of droplet contact angle θ. This is determined by the conservation of mass. Consequently, the change of particle speed $\bar{u}$ depends on how the ratio of D^* to θ changes with time. When the influence on the particle speed, caused by weakening the evaporation-driven flow with the increase of density, is enough to counteract that caused by reducing the contact angle, the particles will definitely be retarded. This is the situation in blended droplet, where the effect of density increase weakening evaporation-driven flow becomes dominant and finally $\bar{u}$ decreases with time.

3.2.2. Emergence of vortexes

In our experiment, another remarkable phenomenon is that vortexes appear in the saline droplet in stage II (see movie S2 in the Supplemental material). The particle speeds in the vortex are much greater than in other region in the droplet. The vortex exits in a limited area, and it only affects the particles in it, which is different from the global ring currents in droplet as mentioned in some papers. The vortex forms when most of the particles in the droplet move towards the edge, and its direction and scale keep evolving after its formation. Generally, one

vortex can be seen in the field of view. But sometimes, symmetrical vortexes are observed. Comparing with this, there is no vortex from beginning to end in pure colloidal droplet. Therefore, the dissolved salt in the droplet is supposed to be a key factor for the formation of vortex.

The effect of salt on vortex formation can come from twosources. One is that the inhomogeneous evaporation of different parts in the droplet brings about a concentration gradient of NaCl, which leads to a density gradient as the concentration of solution is related to its density. If the density gradient is large enough, it will cause a buoyancy-driven flow,[25] which may evolve into a vortex afterwards. The other is that the evaporation rate is faster near the edge of the droplet surface, while it is slower in the center. This uneven local evaporation rate will also lead to a concentration gradient of NaCl along the droplet surface. Generally speaking, the surface tension of a saline droplet increases with the rising of salt concentration,[26] thus a surface tension gradient is generated. This will also cause flows on the surface and in the droplet when the gradient is sufficiently large, which is called the flow driven by Marangoni effect. The vortex can also derive from this kind of flow.

In theory, the two different mechanisms of forming vortex should exist simultaneously. Quantitative comparison of the intensity of the two factors can be made through the discussion of two dimensionless numbers: the Rayleigh number *Ra* which characterizes the strength of the buoyancy effect, and the Marangoni number *Ma* which characterizes the strength of the Marangoni effect. The parameters that affect the values of these two dimensionless numbers remain to be further determined experimentally.

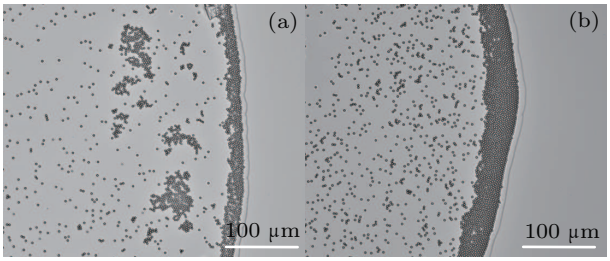


Fig. 4. Deposition morphology of colloidal particles on periphery of (a) saline colloidal droplet (ω(PS) = 0.1%, ω(NaCl) = 0.9%) and (b) pure colloidal droplet.

The dissolved salt in the blended droplet retards the radial migration of particles in stage I, and leads to the vortex to form in stage II, which also disturbs the movement and deposition of colloidal particles. These factors jointly affect the morphology of the ring deposit significantly at the edge of droplet. The coffee-ring morphologies at the boundary of blended droplets and pure colloidal droplets are compared with each other in Fig. 4. It can be seen clearly that in the ring deposit of pure colloidal droplet, the configuration of the particles is more compact, while in the blended droplet it is looser. In addition, the width of coffee-ring deposit in pure colloidal droplet is nearly twice that in blended droplet. Such results indicate that the addition of salt can affect the micro-flow within the droplet during the evaporation, thereby changing the deposition morphology of the colloidal particles.

3.2.3. Influence of growing NaCl crystal on surrounding particles

When the salt in the droplet nucleates and crystallizes, the motion of the colloidal particles around the growing crystal of NaCl is affected more significantly. But if the crystallization happens after all particles have settled, the effect is not conspicuous as the particles are bound to the substrate and restrict their move, which is the case of our experiments above.

In order to observe the effect of salt crystallization, we also carry out the experiments on 20% salt solution droplets. In this case, the solution reaches saturation before all colloidal particles are settled. When the crystal nuclei form and start to grow, the motion trend of the particles in the region adjacent to the grains of salt is changed in different ways (see movie S3 in the Supplemental material). The colloidal particles near the superficial layer or in it are pushed away from the grains. The repulsion effect of the grains has an action range. At a distance which is several times the length of a crystalline grain from the center of this grain, the effect weakens to a low level. The colloidal particles are barely pushed further away at that distance. This is possibly because of a local surface tension gradient which is caused by the gradient of salt concentration near the grains. The regions close to the grains are of a lower concentration as the salt in the droplet is consumed when the NaCl crystal appears and grows up. As discussed by Sghaier *et al.*, surface tension of a saline droplet increases with the salt concentration increasing.[26,27] The liquid surface tension near the NaCl crystal is smaller as shown in Fig. 5.

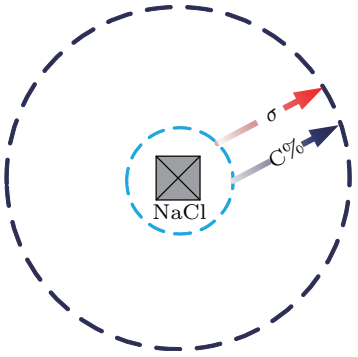


Fig. 5. Influence of NaCl crystal on salt concentration and the surface tension: σ-surface tension, C%-salt concentration.

However, the particles under the superficial layer seem to be affected by the salt grains in different ways. When the crystals grow, a considerable number of colloidal particles under the superficial layer dash quickly towards the grains. Some of them hit the surfaces of the grains and are bounced off, while

some others enter into the gap between the grains and the substrate [see movie S3 in the Supplemental material]. The reason for the unusual flow towards the salt grains is inferred to be a compensation flux caused by the outward flow near the superficial layer.

3.3. Effects of PS colloidal particles on NaCl crystals

The deposition patterns of saline colloidal droplet and pure saline droplet are compared with each other to analyze whether the PS colloidal particles have an effect on the crystallization of NaCl. The mass fraction of NaCl in the droplet is prepared to be 0.9%. The volume of the droplets is kept the same as that in previous experiments.

We first measure the radius of the region of dried deposition with scattered NaCl crystals. The radius of the dried blended droplet, which could be obtained from Fig. 1(j), is about 1.27 mm. By contrast, the radius of the dried pure saline droplet (see Fig. 6) is around 1.20 mm. The shrinkage of diameter in pure saline droplet indicates that its contact line recedes more during evaporation. Further observation reveals the reason for the differences.

It is notable that the coffee-ring formed by the deposited colloidal particles in the blended droplet has a pinning effect on the boundary contact line of the droplet due to the hydrophilia of PS colloidal spheres. When the droplet evaporates, the water cannot separate from the coffee-ring easily even though the receding contact angle generates an inward driving force to the contact line. As a result, the radius of the droplet is stable before the solution reaches saturation. And finally the salt crystallizes in the whole region of droplet, the shape of which is approximately circular and defined by the coffee-ring.

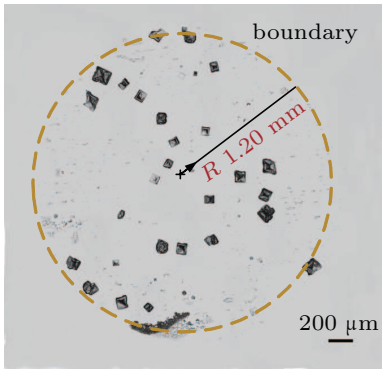


Fig. 6. The morphology of dried deposits in pure saline droplet (ω(NaCl) = 0.9%) and its radius of deposition.

By contrast, the radius of a pure saline droplet keeps decreasing during evaporation as the receding of the contact line is not impeded. When the solution reaches saturation and starts to crystallize, the radius of the droplet has reduced a lot. Thus the eventual crystalline region is smaller. In a word, the range of salt crystallization in saline colloidal droplet is affected by the colloidal particles through pinning the boundary contact line of the droplet.

Moreover, we record the sequential images of stage III in the center of the blended droplet on a smaller scale (see Fig. 7). It can be found that the colloidal particles also work as a factor to control the formation of the salt crystal grains. At sage III, the droplet has shrunk into a thin liquid film. Almost all the particles are settled on the substrate. At this time, an initial crystal has come out as marked by the red arrow in Fig. 7(b), then the liquid film quickly ruptures at a moment as marked by the yellow dashed circle in Fig. 7(c). Subsequently, the gaps expand gradually in the intervals of the settled particles. The liquid film breaks into a mass of patches eventually (some examples are marked with red circles in Fig. 7(e)). Each patch contains several colloidal particles due to the hydrophilia of the particles.

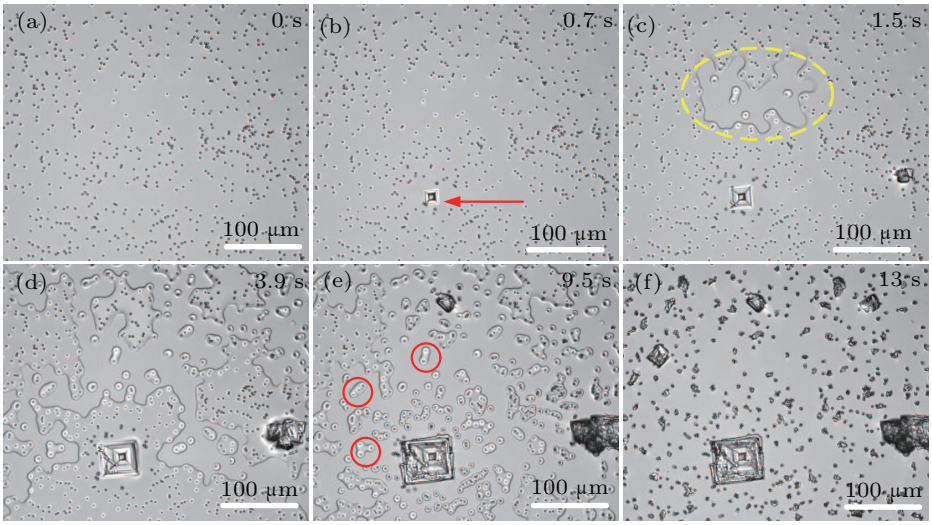


Fig. 7. Last stage of drying in chronological order, showing (a) the continuous thinning of local area of liquid film, (b) the occurring of the first wave of crystals, (c) the rupturing of liquid film, (d) the further rupturing and forming of liquid patches, (e) the occurring of liquid patches and growing up of crystal marked in Fig. 7(b), and (f) resulting overall dried deposits.

Due to the unique role of colloidal particles, the quantity of crystalline grains occurring in the blended droplet depends on how many patches the residual liquid film is divided into. In comparison, in pure saline droplet, the residual liquid film does not break up into so many patches during evaporation because of the lack of colloidal particles. Therefore, the salt mainly separates out on a few initial crystal grains (as shown in Fig. 6). This determines that there are more scattered salt crystal grains in the final deposition patterns of saline colloidal droplet. In addition, the average size of the grains also decreases. Because the salt in the blended droplet is separated into more grains, which leads to less quantity of salt in each one. Accordingly, the colloidal particles have a significant influence on NaCl crystals.

4. Conclusions

We study the different stages of the drying sessile saline colloidal droplets, including the final pattern formation. By comparison and analysis, it is found that the micro-flow in blended droplets is significant affected due to the existence of salt. The evaporation-driven radial compensation flow slows down. In addition, there appear commonly rapid-rotating vortices during the forming stage of coffee-ring. And an outward flow around the growing NaCl crystals is also observed. The gradient of density field and concentration field are considered to be the main reason for the change of micro-flow. On the other hand, it is confirmed that the distribution range and grain size of NaCl crystals are affected by colloidal particles through changing the dewetting process of the residual liquid film. Under the interplay between salt and colloidal particles, the deposition pattern shows obvious differences between the blended droplet and mono-component droplet. The consequences imply that the deposition facies of some biological liquid can be analyzed to acquire important information about its physiological characteristics.

References

[1] Lubarda V A 2012 *Soft Matter* **8** 10288
[2] Weon B M and Je J H 2013 *Phys. Rev. Lett.* **110** 028303
[3] Nikolov A D, Wasan D T, Chengara A, Koczo K, Policello G A and Kolossvary I 2002 *Adv. Colloid Interface* **96** 325
[4] Nikolov A and Wasan D 2014 *Adv. Colloid Interface* **206** 207
[5] Li W B, Lan D and Wang Y R 2017 *Phys. Rev. E* **95** 042607
[6] Yu Y, Zhu H, Frantz J M, Reding M E, Chan K C and Ozkan H E 2009 *Biosyst Eng.* **104** 324
[7] Smalyukh I I, Zribi O V, Butler J C, Lavrentovich O D and Wong G C L 2006 *Phys. Rev. Lett.* **96** 177801
[8] Shatokhina S N, Shabalin V N, Buzoverya M E and Punin V T 2004 *Sci. World J.* **4** 657
[9] Deegan R D, Bakajin O, Dupont T F, Huber G, Nagel S R and Witten T A 1997 *Nature* **389** 827
[10] Wu M M, Man X K and Doi M 2018 *Langmuir* **34** 9572
[11] Yunker P J, Still T, Lohr M A and Yodh A G 2011 *Nature* **476** 308
[12] Fischer B J 2002 *Langmuir* **18** 60
[13] Sefiane K 2014 *Adv. Colloid Interface* **206** 372
[14] Yakhno T A, Yakhno V G, Sanin A G, Sanina O A, Pelyushenko A S, Egorova N A, Terentiev I G, Smetanina S V, Korochkina O V and Yashukova E V 2005 *IEEE Eng. Med. Biol.* **24** 96
[15] Rapis E 2002 *Tech. Phys.* **47** 510
[16] Brutin D, Sobac B, Loquet B and Sampol J 2011 *J. Fluid Mech.* **667** 85
[17] Chen G F and Mohamed G J 2010 *Eur. Phys. J. E* **33** 19
[18] Zhang L, Maheshwari S, Chang H C and Zhu Y X 2008 *Langmuir* **24** 3911
[19] Shahidzadeh-Bonn N, Rafai S, Bonn D and Wegdam G 2008 *Langmuir* **24** 8599
[20] Shahidzadeh N, Schut M F L, Desarnaud J, Prat M and Bonn D 2015 *Sci. Rep-Uk* **5** 10335
[21] Deegan R D, Bakajin O, Dupont T F, Huber G, Nagel S R and Witten T A 2000 *Phys. Rev. E* **62** 756
[22] Soulie V, Karpitschka S, Lequien F, Prene P, Zemb T, Moehwald H and Riegler H 2015 *Phys. Chem. Chem. Phys.* **17** 22296
[23] Marin A G, Gelderblom H, Lohse D and Snoeijer J H 2011 *Phys. Rev. Lett.* **107** 085502
[24] Picknett R G and Bexon R 1977 *J. Colloid Interf Sci.* **61** 336
[25] Kang K H, Lim H C, Lee H W and Lee S J 2013 *Phys. Fluids* **25** 042001
[26] Sghaier N, Prat M and Ben Nasrallah S 2006 *Chem. Eng. J.* **122** 47
[27] Weast R C 1980 *CRC Handbook Chem. Physics*, 61st edn. (CRC Press)